ADVANCED FUNCTIONAL MATERIALS

www.afm-journal.de

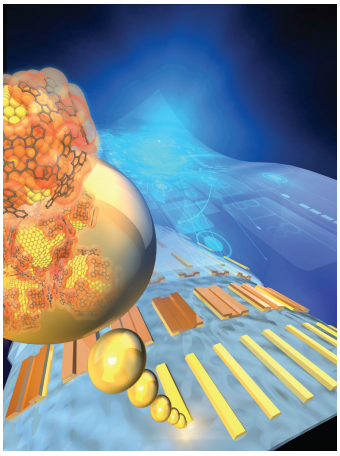

Printed Electronics

T. Minari, M. Kanehara, and co-workers report a method for the room-temperature printing of electronics using gold nanoparticles, enabling semiconductor devices to be printed without the application of heat. On page 4886, organic thin-film transistors are formed on plastic and paper through room-temperature printing, producing devices with mobilities of 7.9 and 2.5 $cm^2 V^{-1} s^{-1}$, respectively. The proposed approach permits the printing of devices on any heat-sensitive substrate, such as plastic, paper, or biomaterials.

Ionene Hydrogels

The topological constraints necessary to enhance hydrogel gelation efficiency are explored by C. Alemán, D. D. Díaz, and co-workers. On page 4893, the performance of hydrogels made from DABCO-containing ionene polymers is studied and compared based on the critical gelation concentration, gelation kinetics, thermal and mechanical stability, optical properties, and dispersion ability for single-walled carbon nanotubes.

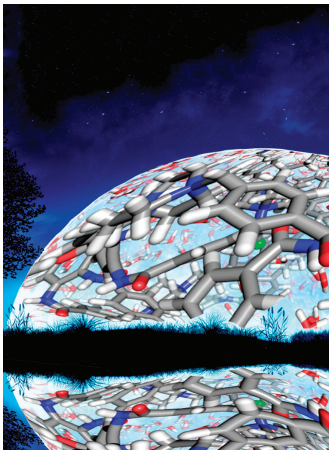

Cellular Solids

Three-dimensional printing of viscoelastic inks is demonstrated by E. B. Duoss, C. M. Spadaccini, T. S. Wilson, and co-workers on page 4905. This technique is shown to create porous, elastomeric architectures with highly controlled mechanical properties, exhibiting markedly distinct load responses with directionally dependent behavior, including negative shear stiffness.

CONTENTS

FULL PAPERS

Graphene

Oxygen-Free Highly Conductive Graphene Papers

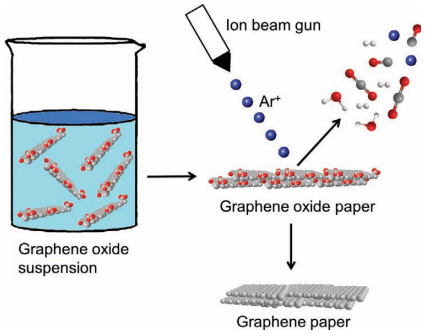

Graphene papers are prepared by irradiation of graphene oxide papers with Ar^+ ion beam. Surface of the paper is chemically reduced and C/O ratios over 100 are achieved. The resulting surface is highly conductive and electrical Ohmic behavior is observed. Gases evolved during irradiation process are also analyzed.

Printed Electronics

Room-Temperature Printing of Organic Thin-Film Transistors with π-Junction Gold Nanoparticles

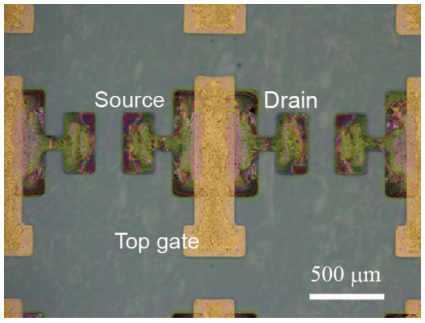

Room-temperature printed electronics are realized as a low-cost, large-area fabrication method for flexible electronic devices. Development of a π-junction gold nanoparticle ink enables the formation of fully printed organic thin-film transistors under atmospheric conditions at room temperature. The printed transistor devices exhibit average field-effect mobilities of 7.9 and 2.5 $cm^2\ V^{-1}\ s^{-1}$ on plastic and paper substrates, respectively.

Ionene Hydrogels

Synergistic Computational-Experimental Approach to Improve Ionene Polymer-Based Functional Hydrogels

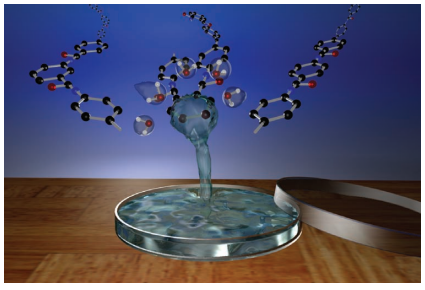

A combined computational-experimental approach identifies the topological constraints necessary to enhance gelation efficiency and achieve superior properties of hydrogels made from DABCO-containing ionene polymers. The best performance of studied ionenes is established based on the critical gelation concentration, gelation kinetics, thermal and mechanical stability, optical properties, and dispersion ability for single-walled carbon nanotubes.

Cellular Solids

Three-Dimensional Printing of Elastomeric, Cellular Architectures with Negative Stiffness

Three-dimensional printing of viscoelastic inks to create porous, elastomeric architectures with mechanical properties governed by the ordered arrangement of their sub-millimeter struts, is reported. Two layouts are patterned, one resembling a "simple cubic"-like structure and another akin to a "face-centered tetragonal" configuration. These mechanical metamaterials exhibit markedly distinct load response with directionally dependent behavior, including negative shear stiffness.

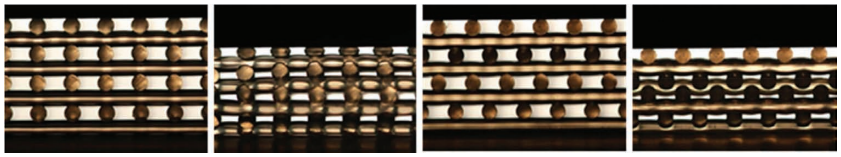

FULL PAPERS

An ultrafast cross-linking method for the fabrication of graphene oxide monoliths (GOM) with poly(oxypropylene) diamines as a cross-linker is reported. This method can form self-assembled 3D GO structures with controllable interlayer spacing. The covalently bonded GOM structure demonstrates high cell viability, could be molded into various shapes, and when hydrated behaves like an elastic hydrogel.

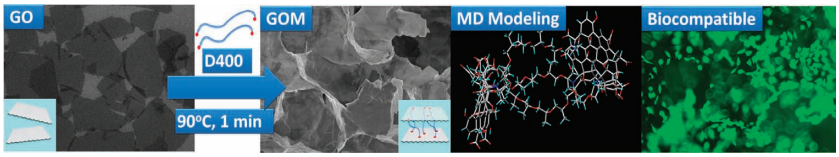

Graphene Oxide

Digital plasmonic patterning (DPP) is developed to mechanically pattern a hydrogel encapsulated with gold nanorods in a digital fashion. DPP can provide orders of magnitude changes in the hydrogel stiffness, and can be tuned by laser intensity and writing speed, in addition to any digital pattern, making it a potentially useful technique for patterning hydrogels for various biomedical applications.

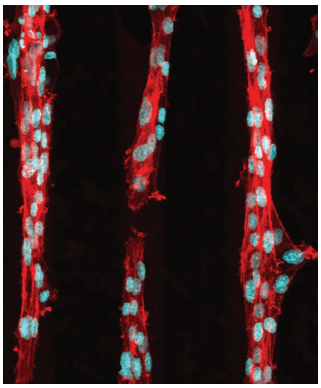

Patterning

Hybrid materials based on wide bandgap GaN and cell membrane models can be operated as an electrochemical charge sensor, which sensitively detects changes in the surface potentials caused by the reversible docking of recombinant proteins to the lipid anchors. By transferring such constructs on quantum dot structures, the potential changes can also be detected by their photoluminescence intensity.

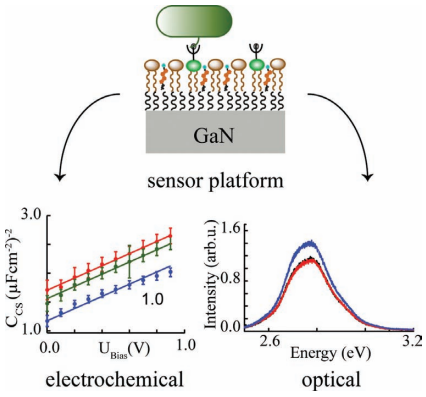

Sensors

By controlling the loading direction, multiple pattern transformations can be induced by buckling in a triangular array of circular holes embedded in an elastic material. Interestingly, these different pattern transformations can be exploited to tune the propagation of elastic waves in the system, enhancing the tunability of its dynamic response.

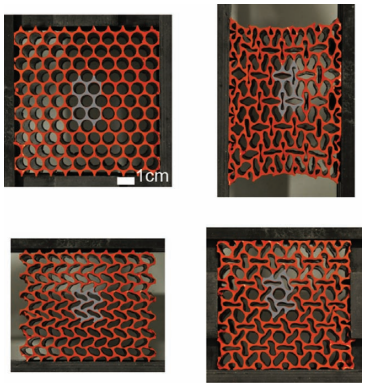

Periodic Structures

CONTENTS

FULL PAPERS

Polymorphism

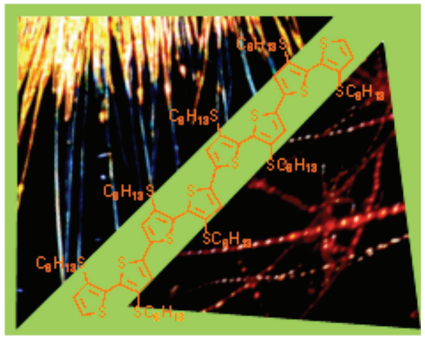

A sulfur overrich octithiophene forms stable polymorphic crystalline microfibers separately and reproducibly grown on glass, ITO, and an interdigitated electrode/SiO_2 surface of a bottom-contact field-effect transistor. The effects of polymorphism on functional properties are reported. DFT calculations suggest the polymorphism to be conformational in nature.

Quantum Dots

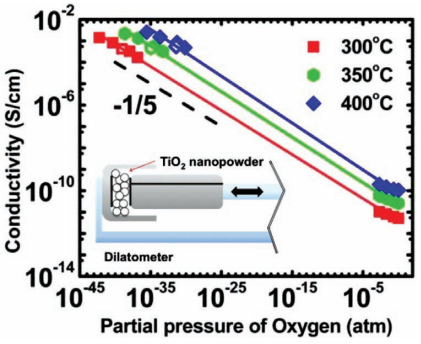

Anatase TiO_2 quantum dots exhibit a Frenkel defect disorder when characterized as loose powder in a modified dilatometer setup, which allows electrical impedance spectroscopy measurements. In addition, lateral expansion indicates necessity of preconditioning to attain equilibrium electronic parameters by eliminating protonic conduction on the surface of the quantum dots.

Field-Effect Transistors

A direct-writing method is used to prepare aligned semiconducting poly(3-butylthiophene) (P3BT) and its blend films with both optical and electrical anisotropy. An increased field-effect mobility of aligned P3BT/polystyrene blends, as compared with neat P3BT, is observed in both vertical and parallel directions. The mobility and threshold voltage are comprehensively tuned, from which a digital inverter with gain up to 80 is realized.

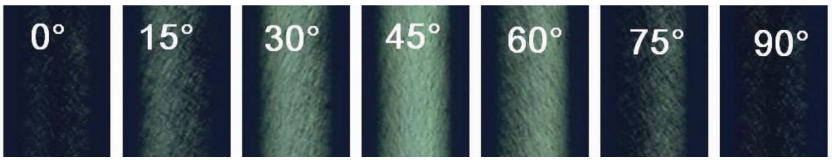

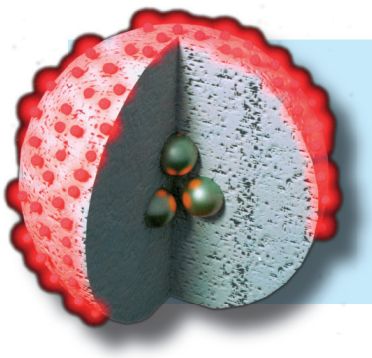

How to contact us:

Editorial Office:
Phone: (+49) 6201-606-286/531
Fax: (+49) 6201-606-500
Email: afm@wiley-vch.de

Reprints:
cherth@wiley-vch.de

Copyright Permission:
Fax: (+49) 6201-606-332
Email: rights@wiley-vch.de

FULL PAPERS

Restacked, layered compounds of graphite, molybdenum disulfide, and boron nitride are ideal materials for electronic devices, censors, and reinforced materials. A high-yielding process using sonochemical fragmentation of precursor powders with antioxidants is performed to generate modified restacked materials. The restacked powders demonstrate unique chemical, thermal, dispersive, and electrical properties that are desirable for polymer composites and other hybrid materials.

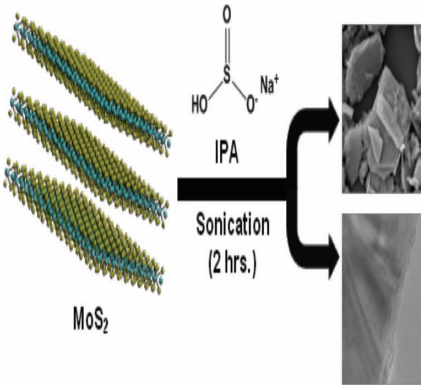

Graphite

Macroscopic Properties of Restacked, Redox-Liquid Exfoliated Graphite and Graphite Mimics Produced in Bulk Quantities

Interface properties of planar hybrid solar cells, PEDOT:PSS/SiO_x/Si, are influenced by the amount of surfactant and co-solvent in PEDOT:PSS. The three-dimensional time-of-flight secondary ion mass spectrometry chemical images reveal a minimal-defect interface for the high efficiency cells, in comparison with more micropore defects at the interface for low efficiency devices. A very high PCE of 13.3% is achieved under optimized conditions.

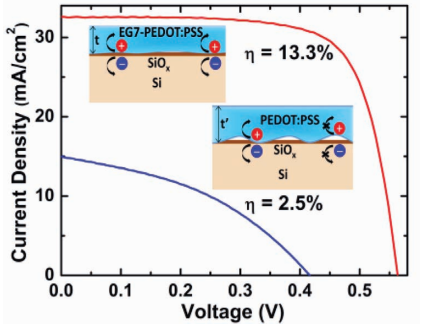

Hybrid Solar Cells

Defect-Minimized PEDOT:PSS/Planar-Si Solar Cell with Very High Efficiency

Deposition of r-graphene oxide (r-GO) onto a glass slide. r-GO sheets stretch upon impact. Pentagonal and heptagonal r-GO sheets undergo bond translation. The resulting "frozen elastic strains" heal the defects (topological defects, namely Stone-Wales and C_2 vacancies) in the r-GO flakes, which is reflected in the reduced ratio of the intensities of the D and G bands in the deposited film.

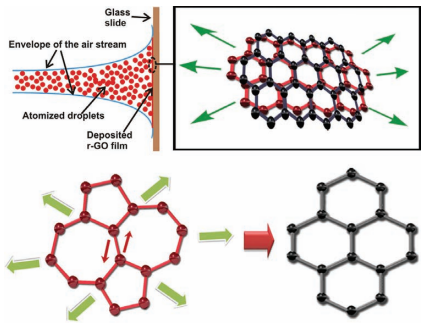

Self-Healing

Self-Healing Reduced Graphene Oxide Films by Supersonic Kinetic Spraying

An originally designed polymer reactor composed of a thermosensitive control layer and an inert substrate layer is reported. With the inert substrate layer made of poly(acrylamide), the thermosensitive control layer consists of nickel nanoparticles and a unique polymer composite of poly(1-vinylimidazole) and poly(acrylic acid) that exhibit thermosensitive interactions. The self-healing and dissociation of the thermosensitive interactions induce convex/concave-switchable shapes in the resulting reactor, which cause tunable access to the encapsulated metal nanoparticles. In this way, this reactor demonstrates tunable catalytic ability.

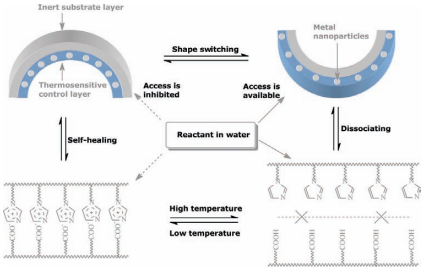

Polymer Reactors

A Catalytic and Shape-Memory Polymer Reactor

FULL PAPERS

Hybrid Nanostructures

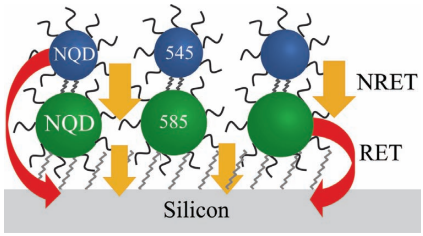

Size-gradient CdSe/ZnS nanocrystal bilayer structures are fabricated on Si substrates in a layer-by-layer architecture with assistance of chemical linkers. Efficient energy transfer is demonstrated from photoexcited nanocrystals into the substrate as achieved via cascaded nonradiative and direct radiative couplings. This supports the concept of excitonic sensitization of ultrathin Si layers from the adjacent nanocrystal assemblies for photovoltaic applications.

Biosensors

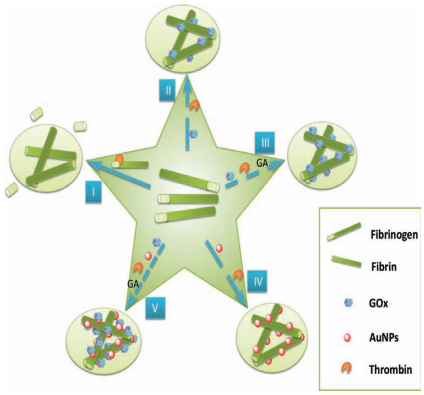

Inspired by blood coagulation, fibrin-boned bionanocomposites are presented as efficient matrices of biomacromolecules and nanomaterials for biosensing applications. The fibrin-boned networks show promising properties, endowing the bionanocomposites with high efficiency in capturing Au nanoparticles, magnetic nanoparticles, and glucose oxidase, even at 99%, 98%, and 57%, respectively, as well as significant mass-transfer and biocatalysis efficiencies.